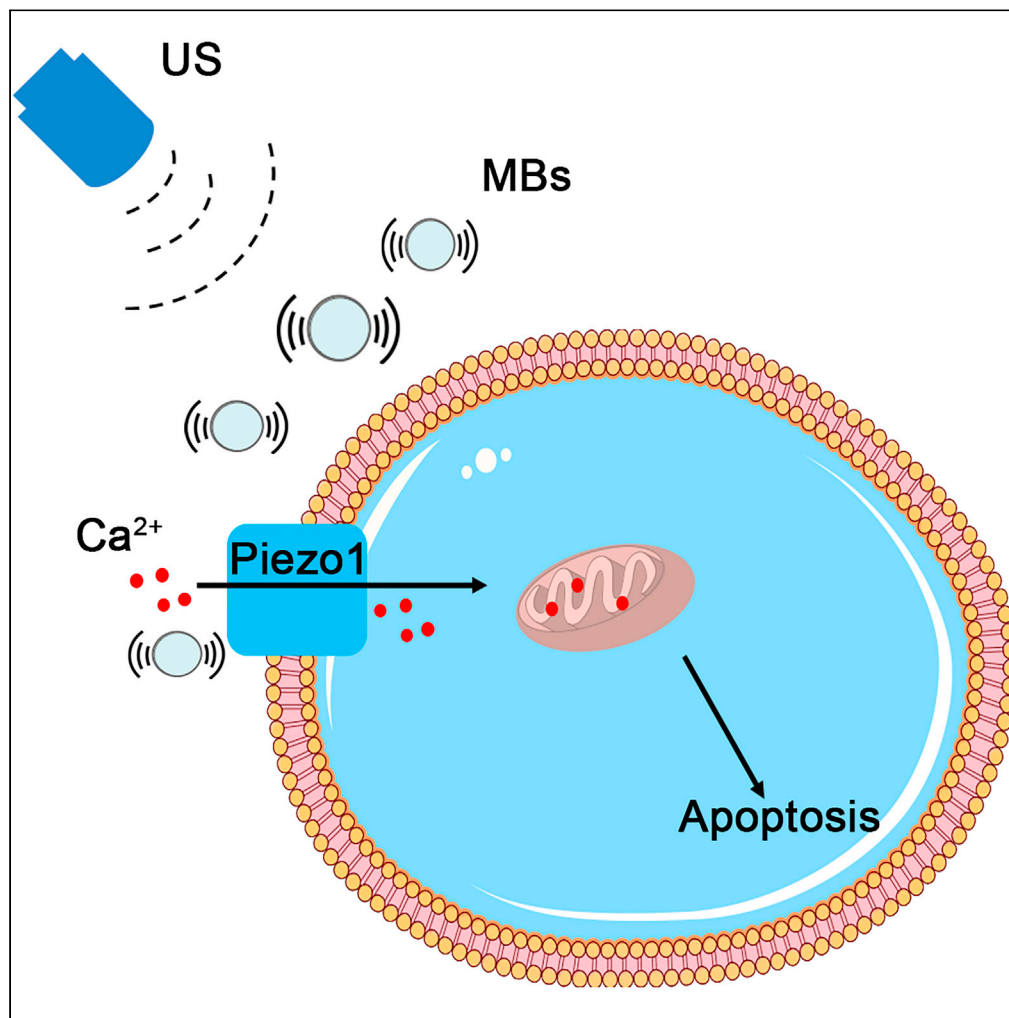**Article**

Mechanosensitive channel Piezo1 induces cell apoptosis in pancreatic cancer by ultrasound with microbubbles

Yue Song, Jifan Chen, Cong Zhang, ..., Chao Zhang, Shiyan Li, Pintong Huang

lishiyan@zju.edu.cn (S.L.)
huangpintong@zju.edu.cn (P.H.)

Highlights

Mechanosensitive channel Piezo1 is highly expressed in pancreatic cancer cells

Ultrasound with microbubbles induces apoptosis of pancreatic cancer cells

Piezo1 is activated by ultrasound with microbubbles and mediates calcium influx

Article

Mechanosensitive channel Piezo1 induces cell apoptosis in pancreatic cancer by ultrasound with microbubbles

Yue Song,[1,2,4] Jifan Chen,[1,2,4] Cong Zhang,[1,2] Lei Xin,[1,2] Qunying Li,[1,2] Yajing Liu,[1,2] Chao Zhang,[1,2] Shiyan Li,[3,*] and Pintong Huang[1,2,5,*]

SUMMARY

Ultrasound (US), as a safe and non-invasive tool, has drawn researchers' attention to treat pancreatic ductal adenocarcinoma (PDAC). Piezo1, a mechanosensitive channel, can be activated by various mechanical stimuli. In this study, we tested the expression of Piezo1 in PDAC cell lines and tissues, and cell apoptosis *in vitro* and *in vivo* with siRNA, a lentivirus system, and a subcutaneous xenograft tumor-bearing model under the condition of US with microbubbles (MBs). We found that Piezo1 was highly expressed in PDAC cells; it was activated by US with MBs and was closely related to the apoptosis of PDAC cell lines and tumors. This study highlighted the idea of utilizing the high expression of Piezo1 in PDAC and US with MBs to provide a non-invasive strategy for the treatment of PDAC from the aspect of mechanotransduction.

INTRODUCTION

Pancreatic cancer is considered one of the most life-threatening cancers, of which about 90% is pancreatic ductal adenocarcinoma (PDAC). Patients with PDAC suffer from locally advanced disease and extreme desmoplasia (Humphris et al., 2014), which are the main reasons they lose the opportunity for radical resection and exhibit insensitivity to chemotherapy or radiotherapy. Moreover, chemotherapy and radiotherapy often cause undesirable systemic side effects. Thus, exploring alternative treatments is imperative.

One study reported commercially available ultrasound (US) combined with microbubbles (MBs) enhanced the efficacy of gemcitabine and increased the median survival of patients with PDAC from 8.9 months to 17.6 months. Thus, relative to traditional therapies, US has gained interest as a high-potential treatment for pancreatic cancer (Dimcevski et al., 2016). Sonoporation played a role in this research. Cavitation, a process in which MBs form and collapse with changes of the local pressure, is another important effect of US with MBs (Kooiman et al., 2014; Lentacker et al., 2014; Wu and Nyborg, 2008). Several studies have demonstrated that US with MBs caused apoptosis of colon cancer, hepatic tumors, and pancreatic cancer, as well as suppressed the tumor invasion of pancreatic cancer cells. However, the underlying mechanisms were not thoroughly studied (Cao et al., 2021; Huang et al., 2013; Li et al., 2016; Sun et al., 2018; Suzuki et al., 2016; Zhang et al., 2014).

Research on the interaction of US with mechanosensitive channels (MSCs) has drawn wide attention. MSCs can sense and respond to various internal or external mechanical stimuli, including shear stress induced by ultrasonic stimulation (Perozo and Rees, 2003). Mammalian MSCs, Piezo1, and Piezo2 were cloned in 2010 (Coste et al., 2010, 2012). Piezo1, a non-selective cation channel inclined to transfer Ca^{2+}, was initially reported to be highly associated with embryonic development and sensing shear stress (Bagriantsev et al., 2014; Coste et al., 2012; Zhang et al., 2017). For acute respiratory distress syndrome, Piezo1 was related to apoptosis of type II pneumocytes (Liang et al., 2019). For degenerative nucleus pulposus (NP) tissue, Piezo1 was highly expressed and activated by a stiff extracellular matrix and triggered the apoptosis of human NP cells (Wang et al., 2021). For prostate cancer, Piezo1 increased circulatory-shear stress-related TRAIL sensitization and induced significant apoptosis (Hope et al., 2019). However, the role of Piezo1 in the apoptosis of pancreatic cancer cells has rarely been reported.

Ultrasound, a safe external stimulation signal, is suitable for MSCs. The *Escherichia coli* mechanosensitive channel of large conductance precisely activated via US was transfected into rat hippocampal neurons and

[1]Department of Ultrasound in Medicine, The Second Affiliated Hospital of Zhejiang University School of Medicine, Zhejiang University, Hangzhou 310009, China

[2]Research Center of Ultrasound in Medicine and Biomedical Engineering, The Second Affiliated Hospital of Zhejiang University School of Medicine, Zhejiang University, Hangzhou 310009, China

[3]Department of Ultrasound in Medicine, Affiliated Sir Run Run Shaw Hospital of Zhejiang University School of Medicine, Hangzhou 310009P.R. China

[4]These authors contributed equally

[5]Lead contact

*Correspondence: lishiyan@zju.edu.cn (S.L.), huangpintong@zju.edu.cn (P.H.)
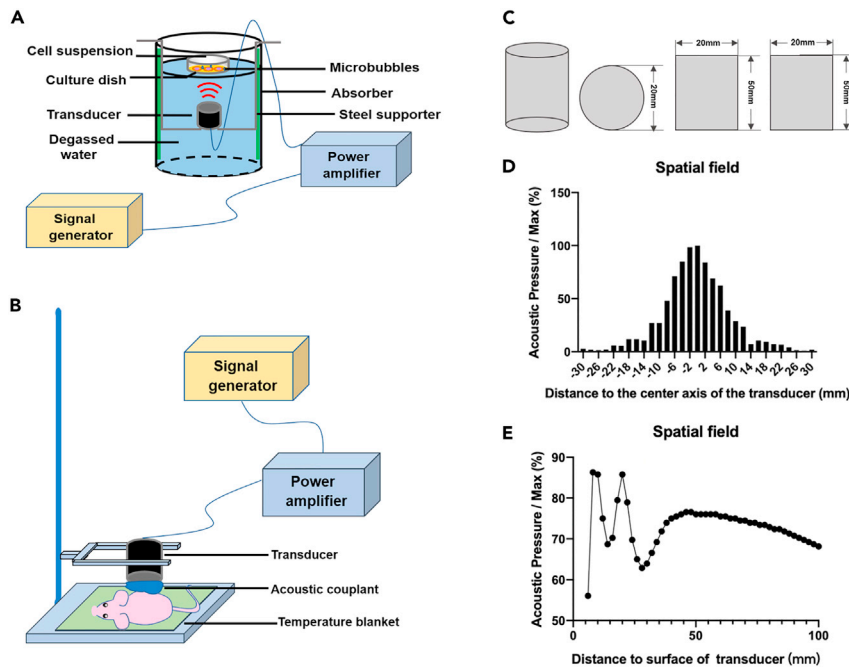
Figure 1. Schematic of the ultrasonic equipment and experimental setup

(A and B) Ultrasonic equipment consisting of a signal generator, a power amplifier, a transducer, a steel supporter, and a tank with degassed water. Transducer was fixed on the steel supporter 5 cm apart from the culture dish.

(C) Three-view diagram of the transducer, which was a cylinder 20 mm in diameter and 50 mm in height.

(D) The acoustic pressure was maximal at the center of the transducer.

(E) The center acoustic pressure became stable and was about 76% of the maximum at a 50 mm distance between the transducer and the culture dish.

triggered nerve action at low acoustic intensity (Ye et al., 2018). *Caenorhabditis elegans* neurons expressing TRP-4 were evoked via US with MBs and led to behavioral outputs (Ibsen et al., 2015). In immunotherapy, Piezo1-integrated T cells cultured with a medium containing Ca^{2+}, when exposed to US with MBs, expressed chimeric antigen receptors and eradicated target Toledo lymphoma tumor cells (Pan et al., 2018).

This study aimed to utilize the high expression of mechanosensitive channel Piezo1 in PDAC to achieve a non-invasive treatment strategy with the help of US with MBs. We evaluated the expression of Piezo1 in pancreatic cancer cell lines, specimens from patients with PDAC, and oncology databases and verified the therapeutic effect *in vitro* and *in vivo*. This study may provide insights into the potential of mechanical transduction in the treatment of PDAC by using US with MBs.

RESULTS

Ultrasonic equipment and spatial field of the transducer

The ultrasonic equipment consisted of a signal generator, a power amplifier, a 1 MHz transducer, and a tank with degassed water (Figures 1A and 1B). The cylindrical transducer measured 20 mm in diameter and 50 mm in height (Figures 1C and S7). The acoustic pressure of the transducer at different distances from its center was measured with a hydrophone; the spatial field showed that it was 100% at the center (Figure 1D). The acoustic pressure at the center was measured, with the transducer positioned at different distances from the culture dish. The data indicated that when the distance was 50 mm, the acoustic pressure became stable and was 76% of the maximum (Figure 1E).

Piezo1 is highly expressed in pancreatic cancer cells and tissues

Western blot analysis showed that the expression of Piezo1 in pancreatic cancer cell lines, particularly BxPC3, was 2.5 folds relative to the normal pancreatic ductal cell line HPNE (Figures 2A and 2B). We
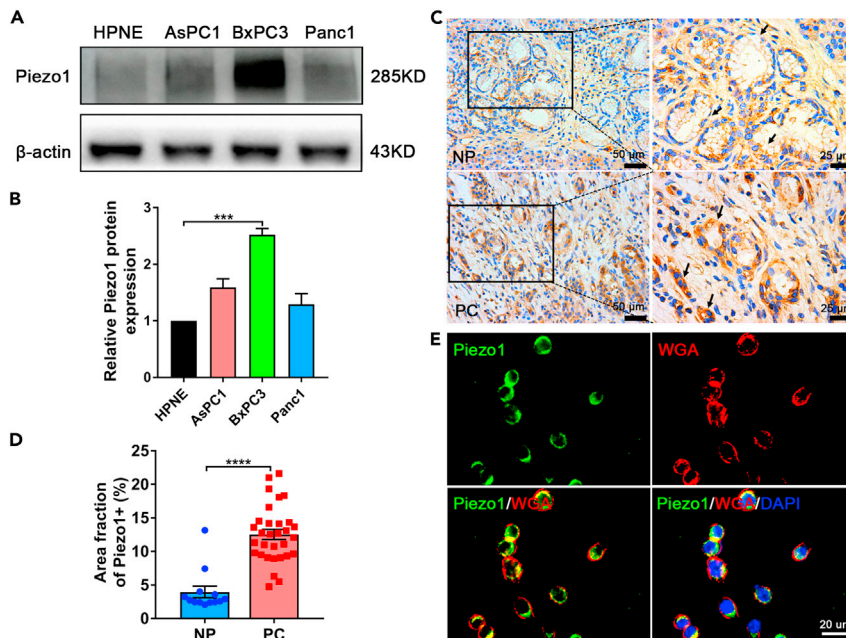
Figure 2. Piezo1 is highly expressed in pancreatic cancer cells and tissues

(A and B) Piezo1 was highly expressed in the BxPC3 pancreatic cancer cell line relative to that in the other two pancreatic cancer cell lines and normal pancreatic ductal cells. Values analyzed from experiments performed at least in triplicate and presented as means ± SEM. ***p<0.001, one-way ANOVA test.

(C and D) Immunohistochemistry showed Piezo1 being abundantly expressed in the pancreatic ductal cells of patients with PDAC relative to that in paired adjacent NP tissues. PC: pancreatic cancer, NP: noncancerous pancreatic. Scale bars: 50 or 25 μm. Black arrows denoted the Piezo1 expression. Values analyzed from experiments performed at least in triplicate and presented as means ± SEM. ****p<0.0001, Student's t-test.

(E) Piezo1 was mainly distributed in the BxPC3 cell membrane, co-localized with the membrane maker WGA as determined by immunofluorescence. Scale bars: 20 μm.

used BxPC3 cell line in all the experiments in our study. Immunohistochemistry also demonstrated that Piezo1 expression in pancreatic cancer tissues was almost threefold the expression in paired adjacent noncancerous tissues (Figures 2C and 2D). Moreover, immunofluorescence indicated that Piezo1 was mainly located in the cytomembrane, with a small amount in the cytoplasm in all three pancreatic cancer cell lines (Figures 2E and S1). Piezo1 was revealed to be highly expressed in pancreatic cancer cells and tissues; in addition, it was mainly located in the cytomembrane.

High expression of Piezo1 is associated with poor survival and patients with advanced clinical stage of pancreatic cancer

To further explore the relationship between Piezo1 expression and clinical outcomes in patients with PDAC, including overall survival (OS), disease-free survival (DFS), clinical stage, and tumor grade, we collected data in the following databases: Oncomine, Gene Expression Omnibus (GEO), Gene Expression Profiling Interactive Analysis (GEPIA), The Cancer Genome Atlas (TCGA), and Kaplan Meier (KM) plotter (http://kmplot.com/). The mRNA level of Piezo1 was increased in patients with both PDAC and pancreatic adenocarcinoma (PAAD) (Figures 3A–3C). No significant difference in OS was found between high- and low-Piezo1 expression groups in the GEPIA database or the KM plotter (Figures 3D and 3F). However, high expression of Piezo1 was correlated with poor DFS in pancreatic cancer cases in both GEPIA and KM plotter databases (p = 0.034 and p = 0.0016, respectively) (Figures 3E and 3G). Datasets collected from GEPIA showed that Piezo1 expression was higher in patients with clinical Stage II than those with Stage I, indicating a close relationship between high Piezo1 expression and advanced clinical stage (Figure 3H). No significant difference was determined in Piezo1 expression between the grades of the tumors (Figure 3I). In summary, the data obtained in the present study clearly indicated that Piezo1 was a potential gene functionally expressed in pancreatic cancer.
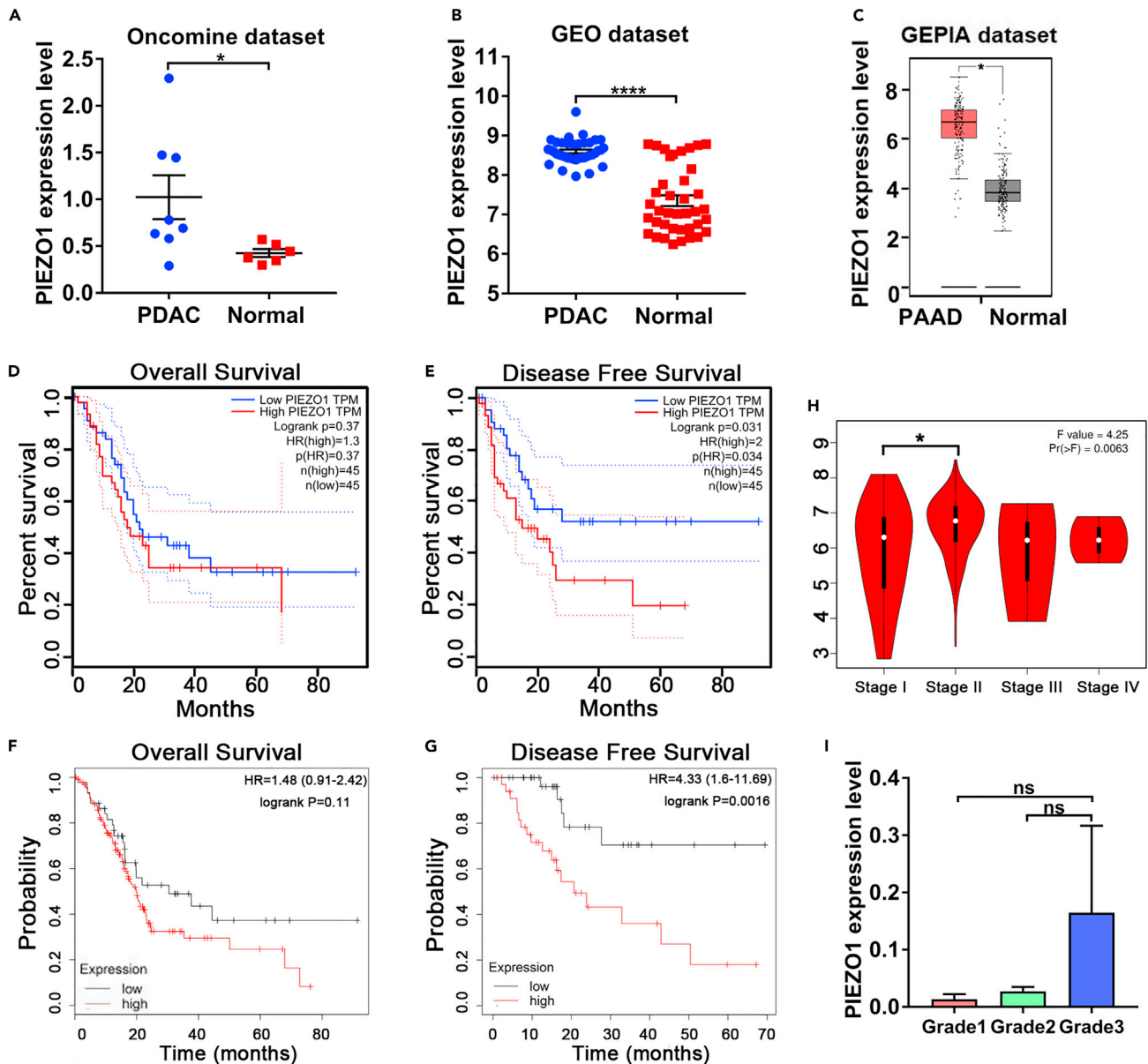
Figure 3. High expression of Piezo1 is associated with poor survival and patients with advanced clinical stage of pancreatic cancer

(A–C) Oncomine, GEO, and GEPIA datasets show that Piezo1 expression was increased in patients with PDAC or PAAD (Oncomine, n = 8 for PDAC *vs.* n = 6 for normal; GEO, n = 39 for PDAC *vs.* n = 39 for normal; GEPIA, n = 179 for PAAD *vs.* n = 171 for normal). Data are represented as mean ± SEM. *p<0.05, ****p<0.0001, Student's *t*-test.

(D–G) GEPIA database and KM plotter showed no significant difference in OS between the high- and low-Piezo1 expression groups (p = 0.37 in GEPIA, p = 0.11 in KM plotter); high Piezo1 expression was closely related to low DFS in pancreatic cancer cases (p = 0.034 in GEPIA, p = 0.0016 in KM plotter).

(H) Piezo1 expression was higher in patients with clinical Stage II than those with Stage I (p = 0.0063; Stage I, n = 21; Stage II, n = 144; Stage III, n = 4; Stage IV, n = 4). Data are represented as mean ± SEM. *p<0.05, one-way ANOVA test.

(I) Piezo1 expression was higher in patients with grade 3 tumor than those with grades 1 and 2 tumor; however, no significant difference was found between these groups.

Piezo1 contributes to apoptosis of pancreatic cancer cells induced by ultrasound with microbubbles

Piezo1, a crucial MSC, is closely related to various biological behaviors of tumors when stimulated by mechanical forces. We explored whether Piezo1 was involved in the apoptosis of pancreatic cancer cells exposed to US. Different US parameters were assessed. The optimal acoustic parameter (acoustic
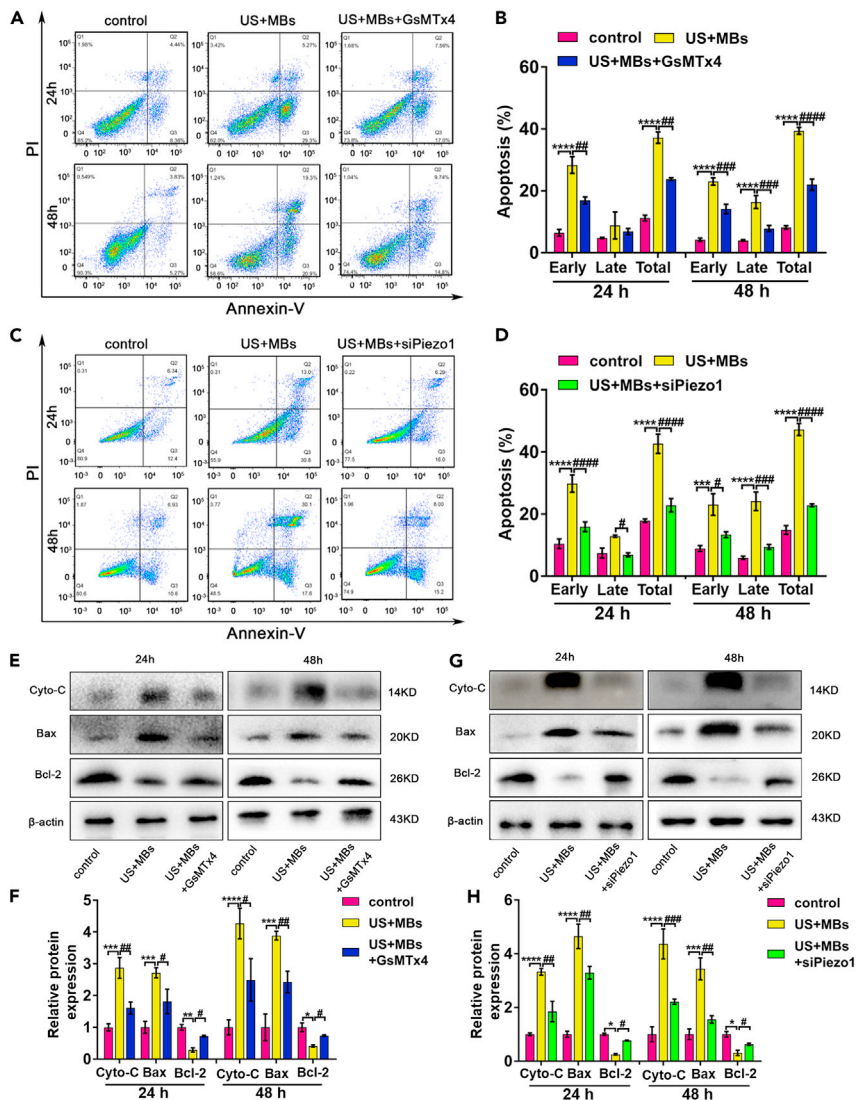
Figure 4. Piezo1 contributes to apoptosis of pancreatic cancer cells induced by ultrasound with microbubbles

(A and B) GsMTx4 alleviated the apoptosis of pancreatic cancer cells induced by US with MBs after incubation for 24 h or 48 h.

(C and D) Partial blockage of Piezo1 by siRNA also alleviated the apoptosis of pancreatic cancer cells when exposed to US with MBs.

(E–H) Western blot analysis showed that the expression of Cyto-C and Bax was increased, whereas that of Bcl-2 was decreased after GsMTx4 or siPiezo1 usage in both 24 h and 48 h groups. All experiments were conducted in triplicate, with the results presented as means ± SEM. *$p < 0.05$, **$p < 0.01$, ***$p < 0.001$, ****$p < 0.0001$, #$p < 0.05$, ##$p < 0.01$, ###$p < 0.001$, ####$p < 0.0001$, two-way ANOVA test.

frequency = 1 MHz; duty cycle = 50%; center SPPA intensity = 1.0 W/cm^2; PNP = 176.377 KPa) that induced cell apoptosis without mechanical damage was ultimately selected (Figure S2). Under this condition, US with MBs induced apoptosis, particularly in the early stage. When the cells were exposed to US with MBs for 10 min and continuously cultured for 24 h and 48 h, respectively, we found that the Piezo1 inhibitor GsMTx4 alleviated total apoptosis by about 36% for the 24 h group (US + MBs: 37.2 ± 1.9%; US + MBs + GsMTx4: 23.8 ± 0.4%) and by 44% for the 48 h group (US + MBs: 39.4 ± 1.1%; US + MBs + GsMTx4: 22.0 ± 1.8%) (Figures 4A and 4B). For the siPiezo1-transfected cells, total apoptosis decreased by 47% and 52% for the 24 h (US + MBs: 42.7 ± 5.4%; US + MBs + siPiezo1: 22.8 ± 3.7%) and 48 h (US + MBs: 47.2 ± 3.3%; US + MBs + siPiezo1: 22.8 ± 0.7%) groups, respectively (Figures 4C and 4D). To further elucidate the mechanism underlying apoptosis, Western blot analysis was used to confirm the expression of

mitochondria pathway-related proteins. Cytochrome *c* and Bax were increased, whereas Bcl-2 was decreased in the US + MBs group. The effect of GsMTx4 or siPiezo1 on protein expression was consistent with the results of flow cytometry (Figures 4E–4H).

Piezo1 contributes to mitochondrial dysfunction of pancreatic cancer cells induced by ultrasound with microbubbles

As earlier demonstrated, US with MBs affected the expression of proteins involved in the pathway of mitochondria-related apoptosis. We further evaluated the mitochondrial functions, including MMP and ATP release, when cells were exposed to US with MBs. JC-1, a fluorescent probe, was used to detect MMP. When apoptosis occurred, MMP decreased, and JC-1 existed as monomers, which were detected as green; otherwise, JC-1 existed as aggregates, which were detected as red. Fluorescence results indicated that in the US + MBs group, JC-1 was mainly green, suggesting the damage of mitochondrial function; GsMTx4 or siPiezo1 increased JC-1 with red fluorescence, particularly in the US + MBs + siPiezo1 group, indicating that Piezo1 blockage alleviated the mitochondrial dysfunction of pancreatic cancer cells caused by US with MBs (Figure 5A). Flow cytometry was then used to quantify JC-1 with green fluorescence—that is, the percentage of the cell population P2 in Figure 5B. GsMTx4 decreased the percentage of JC-1 monomers by about 41% for the 24 h and 48 h groups (24 h US + MBs: $22.0 \pm 0.8\%$; 24 h US + MBs + GsMTx4: $13 \pm 1.3\%$; 48 h US + MBs: $23.6 \pm 1.3\%$; 48 h US + MBs + GsMTx4: $13.8 \pm 1.4\%$) (Figure 5C). For siPiezo1, the percentage was about 50% for both groups (24 h US + MBs: $27.7 \pm 2.7\%$; 24 h US + MBs + siPiezo1: $13.6 \pm 1.1\%$; 48 h US + MBs: $33.6 \pm 1.9\%$; 48 h US + MBs + siPiezo1: $16.7 \pm 1.2\%$) (Figures 5E and 5F). ATP release was significantly reduced when the cells were exposed to US with MBs, and this change was also alleviated by GsMTx4 or siPiezo1 (Figures 5D and 5G). On the basis of the aforementioned results, apoptosis induced by US with MBs was related to mitochondrial dysfunction, and activation of the Piezo1 channel was involved in this process.

Piezo1 partially mediates influx of Ca²⁺ induced by ultrasound with microbubbles in pancreatic cancer cells

Piezo1 preferentially transmits Ca^{2+}, an indispensable second messenger that actively participates in physiopathologic processes, including apoptosis. To confirm the involvement of Ca^{2+} in the apoptosis of pancreatic cancer cells caused by US with MBs, we used the Ca^{2+} probe Fluo-8 AM in the detection of intracellular Ca^{2+} concentration. A medium containing Ca^{2+} was used, and images of cells exposed to US with MBs were captured. US with MBs immediately triggered Ca^{2+} influx, and the fluorescence intensity was decreased in the GsMTx4 and siPiezo1 groups, more so in the latter, indicating that the influx of Ca^{2+} was mediated by the Piezo1 channel when cells were stimulated by US with MBs (Figures 6A and S8). We further detected the fluorescence intensity of Ca^{2+} by flow cytometry; the results confirmed this occurrence (Figure 6B). In summary, Ca^{2+} influx occurred upon exposure of cells to US with MBs, which was mainly ascribed to the activation of the Piezo1 channel by US with MBs.

Knockdown of Piezo1 reduces the therapeutic effect of ultrasound with microbubbles *in vivo*

To further explore the therapeutic potential of Piezo1 *in vivo*, we used BxPC3 cells for the stable knockdown of Piezo1 and the NC to establish a tumor xenograft model. Treatment using US with MBs was administered every other day, and the tumor volume and body weight were measured before every treatment. After treatment with US + MBs, the tumor exhibited delayed growth; however, the growth rate remained higher in the US + MBs + Lv-siPiezo1 group than in the US + MBs + Lv-NC group (Figures 7A and 7C), indicating that the knockdown of Piezo1 weakened the therapeutic effect of US with MBs. On day 13 of the treatment, the smallest tumor volume was observed in the US + MBs + Lv-NC group (Figure 7C). No significant difference in body weight was found between each group (Figure 7B). H&E staining and TUNEL staining were also employed to confirm the apoptosis of resected tumor tissues. H&E staining revealed the shrinkage and fragmentation of the nuclei in the tumor cells and a decrease in tumor cell density in the US + MBs + Lv-NC group (Figure 7C). TUNEL staining exhibited increased green fluorescence intensity in the US + MBs + Lv-NC group, indicating the apoptosis of pancreatic cancer cells (Figures 7C and S6). The combined results prove that Piezo1 also played a role in the apoptosis of cells treated using US with MBs *in vivo*.

DISCUSSION

In the present study, we focused on investigating the potential role of high-expressed Piezo1 in PDAC when cells were exposed to US with MBs *in vitro* and *in vivo*. Piezo1, a protein yet to be thoroughly studied,
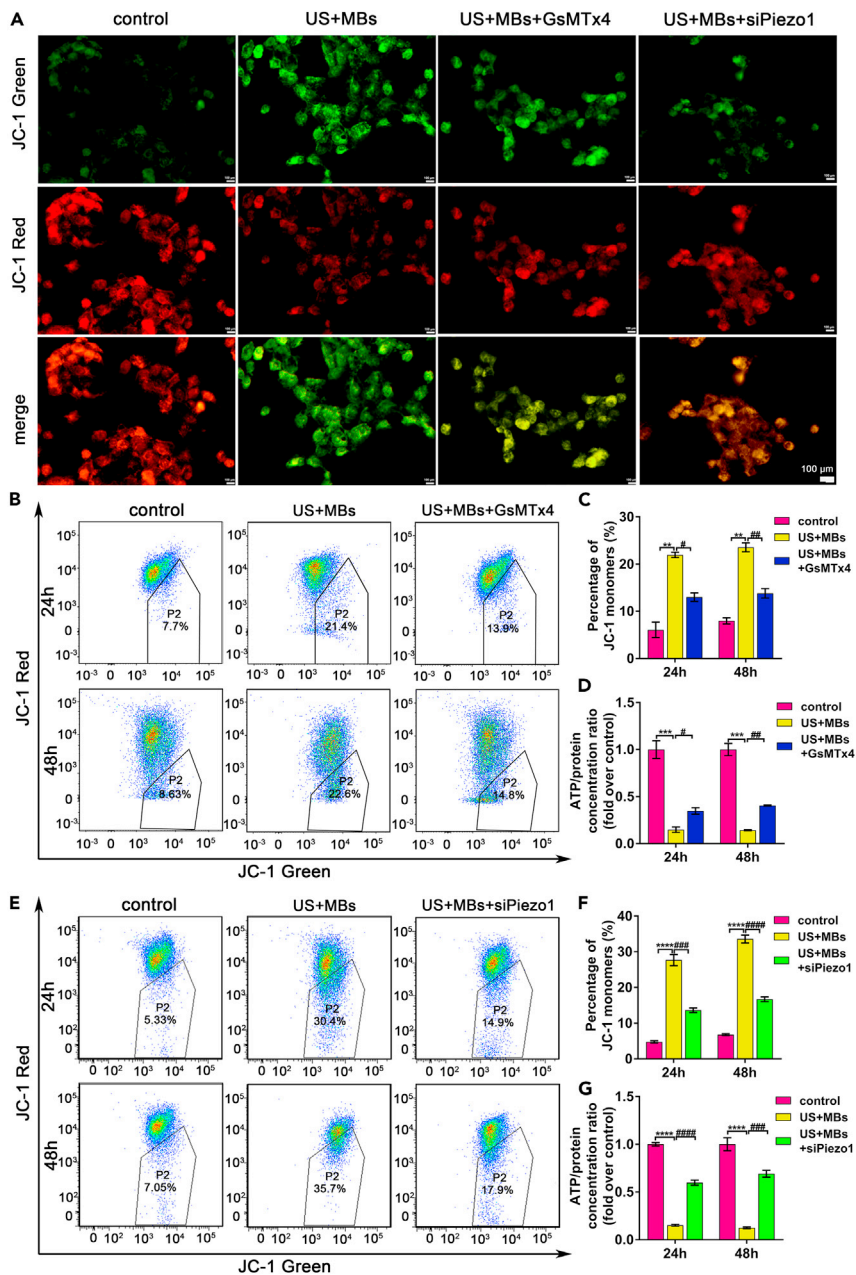
Figure 5. Piezo1 contributes to mitochondrial dysfunction of pancreatic cancer cells induced by ultrasound with microbubbles

(A) The JC-1 dyes exhibiting green and red fluorescence represented the monomers and aggregates of the JC-1, respectively. The JC-1 monomers increased during mitochondrial dysfunction. Both GsMTx4 and siPiezo1 alleviated the production of the JC-1 monomers of pancreatic cancer cells when exposed to US with MBs. Scale bars: 100 μm.

(B, C, E, and F) Flow cytometry showed that the percentage of the JC-1 monomers was increased in the US with MBs group and was alleviated by GsMTx4 or siPiezo1 in both the 24 h and 48 h groups. P2 indicated the percentage of the JC-1 dye exhibiting green fluorescence.

(D and G) ATP production was decreased in the US + MBs group, and GsMTx4 or siPiezo1 partly alleviated this condition for pancreatic cancer cells. All experiments were run in triplicate, with the results presented as means ± SEM. *p<0.05, **p<0.01, ***p<0.001, ****p<0.0001, #p<0.05, ##p<0.01, ###p<0.001, ####p<0.0001, two-way ANOVA test.
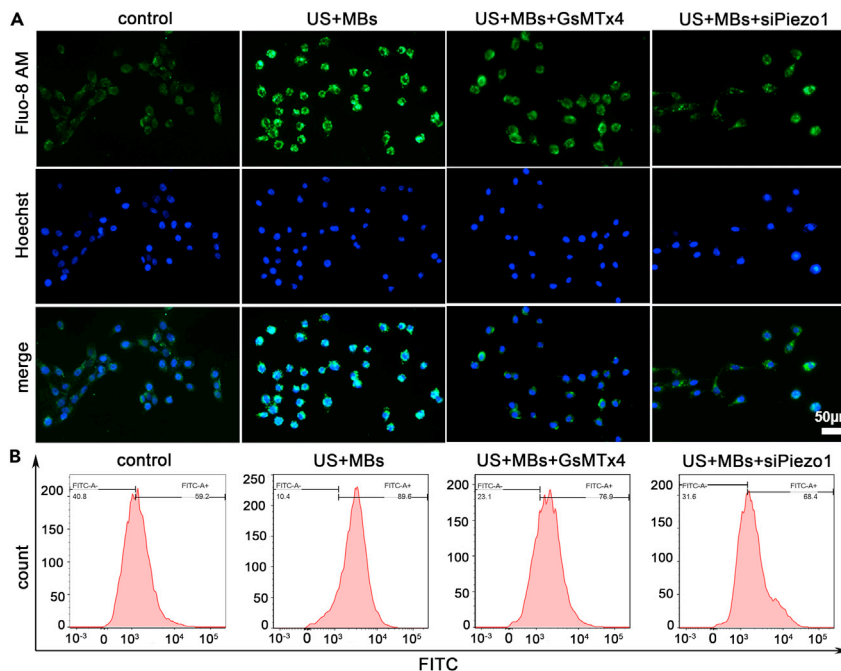
Figure 6. Piezo1 partially mediates influx of Ca²⁺ induced by ultrasound with microbubbles in pancreatic cancer cells

(A) Fluo-8 AM is an indicator of Ca^{2+}. Ca^{2+} influx occurred when the cells were exposed to US with MBs. The use of GsMTx4 or siPiezo1 partly decreased Ca^{2+} influx, but the reduction was more significant in the US + MBs + siPiezo1 group. Scale bar: 50 μm. Hoechst staining was conducted to allow for the fluorescent staining of the cell nucleus.

(B) Cytosolic Ca^{2+} immunofluorescence was measured by flow cytometry and showed similar results.

has a subtle relationship with tumors (Li et al., 2015; Yang et al., 2014; Zhang et al., 2018). Previous studies mainly focused on the role of Piezo1 in lung cancer, gastric cancer, and colon cancer in which its function was heterogeneous (Lentacker et al., 2014; Volkers et al., 2015; Yang et al., 2014). Our preliminary experimental data and oncology databases' results showed that Piezo1 was highly expressed in pancreatic cancer cells, which was closely related to low DFS and patients with advanced clinical stage of PDAC, indicating the potential of Piezo1 as an oncogene in pancreatic cancer. Moreover, Piezo1, as a type of mechanosensitive channel, was activated by US in Piezo1-integrated T cells and eradicated target Toledo lymphoma tumor cells (Pan et al., 2018), prompting us to utilize the high-expressed Piezo1 in pancreatic cancer to achieve therapeutic effect under US with MBs.

We demonstrated cell apoptosis, the expression of apoptosis-related proteins, mitochondrial dysfunction, and elevated Ca^{2+} level in pancreatic cancer cells under US with MBs. GsMTx4 alleviated total apoptosis by about 36% for the 24 h group and 44% for the 48 h group; for siPiezo1, the percentages were 47% and 52%, respectively (Figure 4). The percentage of JC-1 monomers reduced by GsMTx4 was about 41% for the 24 h and 48 h group; for siPiezo1, the percentage was about 50% for both groups (Figure 5). These results indicated that external mechanical stimulation produced by US with MBs contributed to the apoptosis of pancreatic cancer cells via mitochondrial dysfunction, mediated by Ca^{2+}influx partly arising from the activated Piezo1 channel.

The interaction between US with MBs is a highly complicated process involving several factors. Pre-existing stabilized contrast MBs constituted the precondition for cavitation. At a mechanical index (MI) below 0.8, MBs undergo stable cavitation in which MBs oscillate in a symmetric, linear manner but do not collapse (Sirsi and Borden, 2014). Pushing and pulling during the expansion and compression of a stably oscillating MB affected membrane integrity. Pore formation directly allowed calcium to enter the cells. When the MBs repelled the cells, the cell membrane became retracted (Moosavi Nejad et al., 2011). Moreover, MSCs could sense plasma membrane deformation and cytoskeletal rearrangements and transduce these signals into downstream cellular processes, including the mediation of direct Ca^{2+} influx and/or promotion of Ca^{2+}
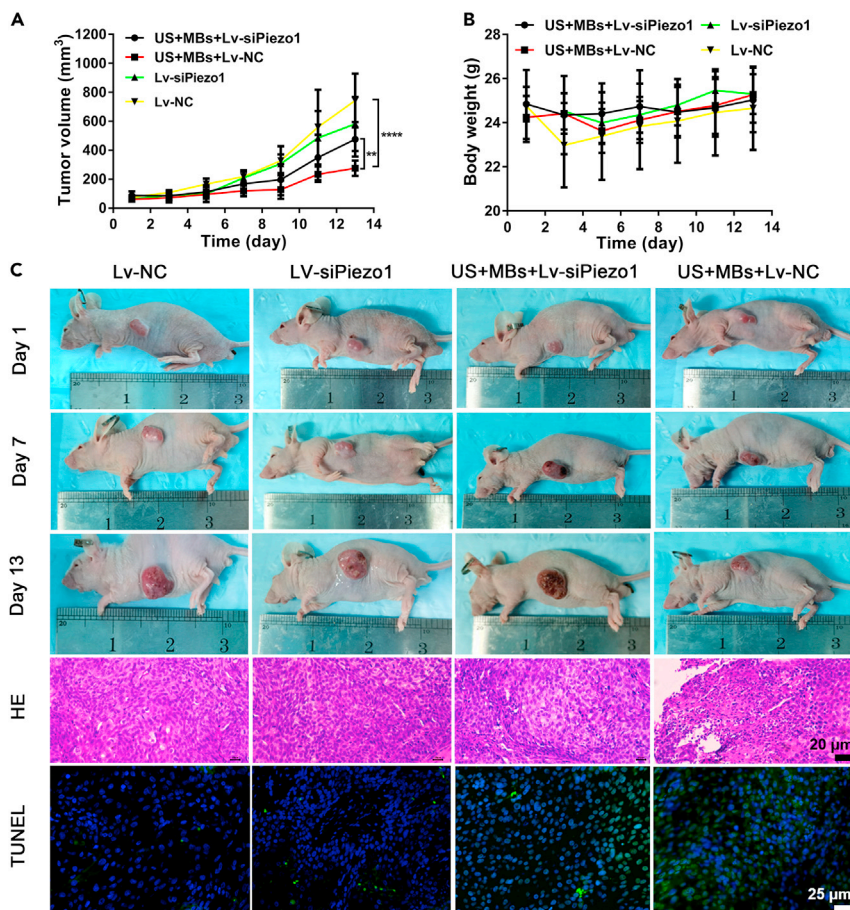
Figure 7. Knockdown of Piezo1 reduces the therapeutic effect of ultrasound with microbubbles *in vivo*

(A and B) Tumor volume and body weight were measured before each treatment conducted every other day. Day 1 represented the first treatment. The US + MBs + Lv-NC group showed the smallest increase in tumor volume.

(C) Representative images of the mouse in each group on days 1, 7, and 13. H&E staining and TUNEL staining showed the extent of cell apoptosis in each group. Scale bars: 20 and 25 μm. Data are presented as the means ± SEM. **p<0.01, ****p<0.0001, two-way ANOVA test.

release from internal stores (Apodaca, 2002). In our study, the cellular apoptosis induced by oscillating MBs under a low-intensity US was partly caused by Piezo1 mediating Ca^{2+} influx.

Although it is not easy to utilize US with MBs *in vivo*, in our study, we chose intratumor injection of MBs before US irradiation. In this way, MBs could loosen the dense tumor stroma under periodic low-intensity US signal and diffuse in the tumor. After treatment using US with MBs, the tumor exhibited slow growth; however, the growth rate was still higher in the US + MBs + Lv-siPiezo1 group than in the US + MBs + Lv-NC group; H&E staining and TUNEL staining also showed severer apoptosis in the latter group (Figure 7), suggesting that the knockdown of Piezo1 weakened the therapeutic effect of US with MBs. In conclusion, the current study highlighted the high expression of Piezo1 in PDAC and utilized its mechanical sensitive feature to treat PDAC. We found and verified the concept that US with MBs stimulated Piezo1-mediated Ca^{2+} influx, mitochondrial dysfunction, and further cellular apoptosis *in vitro* and *in vivo*. With all findings considered, this proof-of-concept study may provide a strategy for the treatment of PDAC from the aspect of mechanotransduction with US with MBs.

In addition, in this study, we chose BxPC3, a wild-type KRAS cell line in all experiments based on the results that the expression of Piezo1 was the highest compared with the other two pancreatic cancer cell lines and normal pancreatic ductal cell HPNE (Figure 2). We did not screen KRAS status in patients with PDAC and explore the relationship between KRAS and Piezo1. For the other two cell lines AsPC1 and PANC1 with

KRAS mutation (Deer et al., 2010), US with MBs also induced apoptosis (Figure S9). About the relationship between KRAS and Piezo1, one research reported EIF3E-RSPO2 and PIEZO1-RSPO2 fusions in colorectal traditional serrated adenoma (TSA) and all the four TSAs with RSPO2 fusions concurrently had KRAS mutations (Hashimoto et al., 2019). But no literatures reported the relationship between KRAS and Piezo1 in pancreatic cancer. The effectors of the Hippo pathway YAP and TAZ (YAP/TAZ) are downstream targets of KRAS and are crucial during cancer initiation and progression in PDAC (Park et al., 2020). Another research reported that the activation of Piezo1 on neural stem cells promoted the nuclear localization of the mechanoreactive transcriptional coactivator YAP and directed the lineage specification (Pathak et al., 2014). These information may give us clues about the relationship between Piezo1 and KRAS. We will do further explore in the future work.

Limitations of the study

The present study has several limitations. Firstly, because MBs are micron-sized, the ideal application of MBs *in vivo* was not very easy. To enhance the therapeutic effect *in vivo*, the liquid-gas phase state change of nano-droplets could make them accumulate in tumors by EPR effect (Maeda et al., 2013). Secondly, Piezo1 overexpression *in vivo* was difficult to achieve because of the high molecular weight of protein. Thirdly, no chemotherapeutic drug or targeted drug was used in our study. Several studies proposed that the combination of US with MBs and siRNA or chemotherapeutic drugs is synergistic in treating cancers and reduces the side effect of chemotherapeutic drugs (Cao et al., 2020). Lastly, because Piezo1 was also expressed in pancreatic stellate cells, an orthotopic model or genetically engineered mouse model of PDAC could be considered in the future work.

STAR★METHODS

Detailed methods are provided in the online version of this paper and include the following:

- KEY RESOURCES TABLE
- RESOURCE AVAILABILITY
  - Lead contact
  - Materials availability
  - Data and code availability
- EXPERIMENTAL MODEL AND SUBJECT DETAILS
  - Cell culture and cell lines
  - Mice
  - Human samples
- METHOD DETAILS
  - Ultrasonic equipment and microbubbles
  - Databases
  - Immunohistochemistry
  - Immunofluorescence
  - Western blot analysis
  - Apoptosis analysis
  - Detection of mitochondrial function
  - Intracellular calcium measurement
  - Cell transfection
  - Pancreatic cancer xenografts and treatment
- QUANTIFICATION AND STATISTICAL ANALYSIS
  - Statistical analysis

SUPPLEMENTAL INFORMATION

Supplemental information can be found online at https://doi.org/10.1016/j.isci.2022.103733.

ACKNOWLEDGMENTS

CellPress
OPEN ACCESS

AUTHOR CONTRIBUTIONS

Y.S. and J.C. designed the experiment. Y.S. and J.C. performed the experiment, analyzed the data, and prepared the manuscript. C.Z. finished the part of bioinformatics analysis in this study. L.X. collected the clinical samples. Q.L., Y.L., and C.Z. supervised the study and contributed in the manuscript revision. S.L. gave valuable guidance on this research. P.H. was responsible for the project administration, supervision, and validation. All authors contributed to this manuscript.

DECLARATION OF INTERESTS

The authors declare no competing interests.

INCLUSION AND DIVERSITY

We worked to ensure diversity in experimental samples through the selection of the cell lines. We worked to ensure diversity in experimental samples through the selection of the genomic datasets.

REFERENCES

Apodaca, G. (2002). Modulation of membrane traffic by mechanical stimuli. Am. J. Physiol. Ren. Physiol *282*, F179–F190. https://doi.org/10.1152/ajprenal.2002.282.2.F179.

Bagriantsev, S.N., Gracheva, E.O., and Gallagher, P.G. (2014). Piezo proteins: regulators of mechanosensation and other cellular processes. J. Biol. Chem. *289*, 31673–31681. https://doi.org/10.1074/jbc.R114.612697.

Cao, J., Hu, C., Zhou, H., Qiu, F., Chen, J., Zhang, J., and Huang, P. (2021). Microbubble-mediated cavitation promotes apoptosis and suppresses invasion in AsPC-1 cells. Ultrasound Med.Biol. *47*, 323–333. https://doi.org/10.1016/j.ultrasmedbio.2020.10.014.

Cao, S., Lin, C., Liang, S., Saw, P.E., and Xu, X. (2020). Enhancing chemotherapy by RNA interference. BIOI *1*, 64–81. https://doi.org/10.15212/bioi-2020-0003.

Coste, B., Mathur, J., Schmidt, M., Earley, T.J., Ranade, S., Petrus, M.J., Dubin, A.E., and Patapoutian, A. (2010). Piezo1 and Piezo2 are essential components of distinct mechanically activated cation channels. Science *330*, 55–60. https://doi.org/10.1126/science.1193270.

Coste, B., Xiao, B., Santos, J.S., Syeda, R., Grandl, J., Spencer, K.S., Kim, S.E., Schmidt, M., Mathur, J., Dubin, A.E., et al. (2012). Piezo proteins are pore-forming subunits of mechanically activated channels. Nature *483*, 176–181. https://doi.org/10.1038/nature10812.

Deer, E.L., González-Hernández, J., Coursen, J.D., Shea, J.E., Ngatia, J., Scaife, C.L., Firpo, M.A., and Mulvihill, S.J. (2010). Phenotype and genotype of pancreatic cancer cell lines. Pancreas *39*, 425–435. https://doi.org/10.1097/MPA.0b013e3181c15963.

Dimcevski, G., Kotopoulis, S., Bjånes, T., Hoem, D., Schjøtt, J., Gjertsen, B.T., Biermann, M., Molven, A., Sorbye, H., McCormack, E., et al. (2016). A human clinical trial using ultrasound and microbubbles to enhance gemcitabine treatment of inoperable pancreatic cancer. J.Control Release *243*, 172–181. https://doi.org/10.1016/j.jconrel.2016.10.007.

Hashimoto, T., Ogawa, R., Yoshida, H., Taniguchi, H., Kojima, M., Saito, Y., and Sekine, S. (2019). EIF3E-RSPO2 and PIEZO1-RSPO2 fusions in colorectal traditional serrated adenoma. Histopathology *75*, 266–273. https://doi.org/10.1111/his.13867.

Hope, J.M., Lopez-Cavestany, M., Wang, W., Reinhart-King, C.A., and King, M.R. (2019). Activation of Piezo1 sensitizes cells to TRAIL-mediated apoptosis through mitochondrial outer membrane permeability. Cell Death Dis *10*, 837. https://doi.org/10.1038/s41419-019-2063-6.

Huang, P., You, X., Pan, M., Li, S., Zhang, Y., Zhao, Y., Wang, M., Hong, Y., Pu, Z., Chen, L., et al. (2013). A novel therapeutic strategy using ultrasound mediated microbubbles destruction to treat colon cancer in a mouse model. Cancer Lett. *335*, 183–190. https://doi.org/10.1016/j.canlet.2013.02.011.

Humphris, J.L., Johns, A.L., Simpson, S.H., Cowley, M.J., Pajic, M., Chang, D.K., Nagrial, A.M., Chin, V.T., Chantrill, L.A., Pinese, M., et al. (2014). Clinical and pathologic features of familial pancreatic cancer. Cancer *120*, 3669–3675. https://doi.org/10.1002/cncr.28863.

Ibsen, S., Tong, A., Schutt, C., Esener, S., and Chalasani, S.H. (2015). Sonogenetics is a non-invasive approach to activating neurons in Caenorhabditis elegans. Nat. Commun. *6*, 8264. https://doi.org/10.1038/ncomms9264.

Kooiman, K., Vos, H.J., Versluis, M., and de Jong, N. (2014). Acoustic behavior of microbubbles and implications for drug delivery. Adv. Drug Deliv. Rev. *72*, 28–48.

Lentacker, I., De Cock, I., Deckers, R., De Smedt, S.C., and Moonen, C.T. (2014). Understanding ultrasound induced sonoporation: definitions and underlying mechanisms. Adv. Drug Deliv. Rev. *72*, 49–64. https://doi.org/10.1016/j.addr.2014.03.003.

Li, C., Rezania, S., Kammerer, S., Sokolowski, A., Devaney, T., Gorischek, A., Jahn, S., Hackl, H., Groschner, K., Windpassinger, C., et al. (2015). Piezo1 forms mechanosensitive ion channels in the human MCF-7 breast cancer cell line. Sci. Rep. *5*, 8364. https://doi.org/10.1038/srep08364.

Li, Y., Wang, P., Chen, X., Hu, J., Liu, Y., Wang, X., and Liu, Q. (2016). Activation of microbubbles by low-intensity pulsed ultrasound enhances the cytotoxicity of curcumin involving apoptosis induction and cell motility inhibition in human breast cancer MDA-MB-231 cells. Ultrason.Sonochem. *33*, 26–36. https://doi.org/10.1016/j.ultsonch.2016.04.012.

Liang, G.P., Xu, J., Cao, L.L., Zeng, Y.H., Chen, B.X., Yang, J., Zhang, Z.W., and Kang, Y. (2019). Piezo1 induced apoptosis of type II pneumocytes during ARDS. Respir.Res. *20*, 118. https://doi.org/10.1186/s12931-019-1083-1.

Maeda, H., Nakamura, H., and Fang, J. (2013). The EPR effect for macromolecular drug delivery to solid tumors: improvement of tumor uptake, lowering of systemic toxicity, and distinct tumor imaging in vivo. Adv. Drug Deliv. Rev. *65*, 71–79. https://doi.org/10.1016/j.addr.2012.10.002.

Moosavi Nejad, S., Hosseini, S.H., Akiyama, H., and Tachibana, K. (2011). Optical observation of cell sonoporation with low intensity ultrasound.

Biochem.Biophys. Res. Commun. *413*, 218–223. https://doi.org/10.1016/j.bbrc.2011.08.072.

Pan, Y., Yoon, S., Sun, J., Huang, Z., Lee, C., Allen, M., Wu, Y., Chang, Y.J., Sadelain, M., Shung, K.K., et al. (2018). Mechanogenetics for the remote and noninvasive control of cancer immunotherapy. Proc. Natl. Acad. Sci. U S A. *115*, 992–997. https://doi.org/10.1073/pnas.1714900115.

Park, J., Eisenbarth, D., Choi, W., Kim, H., Choi, C., Lee, D., and Lim, D.S. (2020). YAP and AP-1 cooperate to initiate pancreatic cancer development from ductal cells in mice. Cancer Res. *80*, 4768–4779. https://doi.org/10.1158/0008-5472.CAN-20-0907.

Pathak, M.M., Nourse, J.L., Tran, T., Hwe, J., Arulmoli, J., Le, D.T., Bernardis, E., Flanagan, L.A., and Tombola, F. (2014). Stretch-activated ion channel Piezo1 directs lineage choice in human neural stem cells. Proc. Natl. Acad. Sci. U S A. *111*, 16148–16153. https://doi.org/10.1073/pnas.1409802111.

Perozo, E., and Rees, D.C. (2003). Structure and mechanism in prokaryotic mechanosensitive channels. Curr.Opin.Struct. Biol. *13*, 432–442. https://doi.org/10.1016/s0959-440x(03)00106-4.

Rhodes, D.R., Yu, J., Shanker, K., Deshpande, N., Varambally, R., Ghosh, D., Barrette, T., Pandey, A., and Chinnaiyan, A.M. (2004). ONCOMINE: a cancer microarray database and integrated data-mining platform. Neoplasia *6*, 1–6. https://doi.org/10.1016/s1476-5586(04)80047-2.

Romac, J.M., Shahid, R.A., Swain, S.M., Vigna, S.R., and Liddle, R.A. (2018). Piezo1 is a mechanically activated ion channel and mediates pressure induced pancreatitis. Nat. Commun. *9*, 1715. https://doi.org/10.1038/s41467-018-04194-9.

Sirsi, S.R., and Borden, M.A. (2014). State-of-the-art materials for ultrasound-triggered drug delivery. Adv. Drug Deliv. Rev. *72*, 3–14. https://doi.org/10.1016/j.addr.2013.12.010.

Sun, Y., Luo, J., Chen, J., Xu, F., Ding, X., and Huang, P. (2018). Ultrasound-mediated microbubbles destruction for treatment of rabbit VX2 orthotopic hepatic tumors. Appl. Acoust. *138*, 216–225. https://doi.org/10.1016/j.apacoust.2018.04.007.

Suzuki, N., Hanmoto, T., Yano, S., Furusawa, Y., Ikegame, M., Tabuchi, Y., Kondo, T., Kitamura, K., Endo, M., Yamamoto, T., et al. (2016). Low-intensity pulsed ultrasound induces apoptosis in osteoclasts: fish scales are a suitable model for the analysis of bone metabolism by ultrasound. Comp. Biochem. Physiol. A. Mol. Integr. Physiol. *195*, 26–31. https://doi.org/10.1016/j.cbpa.2016.01.022.

Tang, Z., Li, C., Kang, B., Gao, G., Li, C., and Zhang, Z. (2017). GEPIA: a web server for cancer and normal gene expression profiling and interactive analyses. Nucleic Acids Res. *45*, W98–W102. https://doi.org/10.1093/nar/gkx247.

Volkers, L., Mechioukhi, Y., and Coste, B. (2015). Piezo channels: from structure to function. Pflugers Arch. *467*, 95–99. https://doi.org/10.1007/s00424-014-1578-z.

Wang, B., Ke, W., Wang, K., Li, G., Ma, L., Lu, S., Xiang, Q., Liao, Z., Luo, R., Song, Y., et al. (2021). Mechanosensitive ion channel Piezo1 activated by matrix stiffness regulates oxidative stress-induced senescence and apoptosis in human intervertebral disc degeneration. Oxid Med.Cell Longev *2021*, 8884922. https://doi.org/10.1155/2021/8884922.

Wu, J., and Nyborg, W.L. (2008). Ultrasound, cavitation bubbles and their interaction with cells.

Adv. Drug Deliv. Rev. *60*, 1103–1116. https://doi.org/10.1016/j.addr.2008.03.009.

Xue, R.Q., Sun, L., Yu, X.J., Li, D.L., and Zang, W.J. (2017). Vagal nerve stimulation improves mitochondrial dynamics via an M(3) receptor/CaMKKβ/AMPK pathway in isoproterenol-induced myocardial ischaemia. J.Cell Mol. Med. *21*, 58–71. https://doi.org/10.1111/jcmm.12938.

Yang, X.N., Lu, Y.P., Liu, J.J., Huang, J.K., Liu, Y.P., Xiao, C.X., Jazag, A., Ren, J.L., and Guleng, B. (2014). Piezo1 is as a novel trefoil factor family 1 binding protein that promotes gastric cancer cell mobility in vitro. Dig. Dis. Sci. *59*, 1428–1435. https://doi.org/10.1007/s10620-014-3044-3.

Ye, J., Tang, S., Meng, L., Li, X., Wen, X., Chen, S., Niu, L., Li, X., Qiu, W., Hu, H., et al. (2018). Ultrasonic control of neural activity through activation of the mechanosensitive channel MscL. Nano Lett. *18*, 4148–4155. https://doi.org/10.1021/acs.nanolett.8b00935.

Zhang, C., Huang, P., Zhang, Y., Chen, J., Shentu, W., Sun, Y., Yang, Z., and Chen, S. (2014). Anti-tumor efficacy of ultrasonic cavitation is potentiated by concurrent delivery of anti-angiogenic drug in colon cancer. Cancer Lett. *347*, 105–113. https://doi.org/10.1016/j.canlet.2014.01.022.

Zhang, J., Zhou, Y., Huang, T., Wu, F., Liu, L., Kwan, J.S.H., Cheng, A.S.L., Yu, J., To, K.F., and Kang, W. (2018). PIEZO1 functions as a potential oncogene by promoting cell proliferation and migration in gastric carcinogenesis. Mol. Carcinog *57*, 1144–1155. https://doi.org/10.1002/mc.22831.

Zhang, T., Chi, S., Jiang, F., Zhao, Q., and Xiao, B. (2017). A protein interaction mechanism for suppressing the mechanosensitive Piezo channels. Nat. Commun. *8*, 1797. https://doi.org/10.1038/s41467-017-01712-z.

STAR★METHODS

KEY RESOURCES TABLE

REAGENT or RESOURCE	SOURCE	IDENTIFIER
Antibodies		
Piezo1	Proteintech	Cat# 15939-1-AP; RRID:AB_2231460
beta actin	Abcam	Cat# ab8226; RRID:AB_306371
Cytochrome C	Cell Signaling Technology	Cat# 11940; RRID:AB_2637071
Bax	Cell Signaling Technology	Cat# 5023 ; RRID:AB_10557411
Bcl-2	Cell Signaling Technology	Cat# 3498 ; RRID:AB_1903907
Biological samples		
Human pancreatic cancer samples from	The Second Affiliated Hospital of Zhejiang University School of Medicine	For patient information, see Table S1
Chemicals, Peptides, and Recombinant Proteins		
GsMTx4	Abcam	Cat# 141871
wheat germ agglutinin	Invitrogen	Cat# W32464
DAPI	Sigma	Cat# D9542
Fluo-8 AM	AAT Bioquest	Cat# 21080
Hoechst	Merck	Cat# 94403
Lipofectamine 6000	Beyotime	Cat# C0526
Critical commercial assays		
Elite Vectastain avidin–biotin complex–peroxidase kit	Vector	Cat# PK-6100
Annexin V–FITC/PI staining kit	BD Biosciences	Cat# 556547
JC-1 staining kit	Beyotime	Cat# C2003S
TUNEL staining kit	Roche	Cat# 11684795910
Experimental models: Cell lines		
AsPC1	ATCC	Cat# CRL-1682 ; RRID:CVCL_0152
BxPC3	ATCC	Cat# CRL-1687 ; RRID:CVCL_0186
PANC1	ATCC	Cat# CRL-1469 ; RRID:CVCL_0480
HPNE	ATCC	Cat# CRL-4023 ; RRID:CVCL_C466
Experimental models: Organisms/strains		
Mouse: BALB/c nude males, 5 weeks old	Beijing Vital River Laboratory Animal Technology	N/A
Software and algorithms		
Fiji-ImageJ	National Institute of Health	https://imagej.net/Fiji; RRID:SCR_003070
FlowJo v10.0	Tree Star	https://www.flowjo.com/solutions/flowjo; RRID:SCR_008520
GraphPad Prism 8	GraphPad	https://www.graphpad.com/ scientificsoftware/prism/; RRID:SCR_002798
SPSS 23.0	SPSS	https://www.ibm.com/analytics/ spss-statisticssoftware; RRID:SCR_002865

(Continued on next page)

REAGENT or RESOURCE	SOURCE	IDENTIFIER
Continued		
Other		
FACSCanto II flow cytometry	BD Biosciences	N/A
Multiscan Spectrum	Molecular Device	N/A

RESOURCE AVAILABILITY

Lead contact

Further information and requests for resources and reagents should be directed to and will be fulfilled by the lead contact, Pintong Huang (huangpintong@zju.edu.cn).

Materials availability

This study did not generate new unique reagents.

Data and code availability

- Data reported in this paper will be shared by the lead contact upon request.

- This paper does not report original code.

- Any additional information required to reanalyze the data reported in this paper is available from the lead contact upon request.

EXPERIMENTAL MODEL AND SUBJECT DETAILS

Cell culture and cell lines

The human pancreatic cancer cell lines AsPC1 (ATCC Cat# CRL-1682, RRID:CVCL_0152), BxPC3 (ATCC Cat# CRL-1687, RRID:CVCL_0186), PANC1 (ATCC Cat# CRL-1469, RRID:CVCL_0480), and normal pancreatic ductal cells HPNE (ATCC Cat# CRL-4023, RRID:CVCL_C466) were cultured in RPMI-1640 (AsPC1, BxPC3) or DMEM (PANC1, HPNE) culture medium (HyClone, Logan, UT, USA) with 10% fetal bovine serum (Gibco, Grand Island, NY, USA) in a humidified incubator at 37°C with 5% (v/v) CO_2 in the air. To block Piezo1, GsMTx4 (Abcam, Cat# 141871, Cambridge, UK) was added to the medium with a final concentration of 2.5 μM (Romac et al., 2018) for at least 1 h.

Mice

The animal experiments in this study were approved and reviewed by the ethics committee of The Second Affiliated Hospital of Zhejiang University School of Medicine (Hangzhou, China). Care and handling of the animals adhered to the guidelines for Institutional and Animal Care and Use Committees. BALB/c male nude mice aged 5 weeks were purchased from Beijing Vital River Laboratory Animal Technology Co., Ltd. (Beijing, China).

Human samples

A total of 30 self-paired tumors and matched noncancerous tissues were obtained from PDAC patients undergoing pancreatectomy before chemotherapy. The histopathology of the specimens was confirmed by pathologic analysis. Informed consent was obtained from each patient, and the study was approved by the ethics committee of The Second Affiliated Hospital of Zhejiang University School of Medicine (Hangzhou, China). The patient information was displayed in Table S1.

METHOD DETAILS

Ultrasonic equipment and microbubbles

The ultrasonic equipment is consisted of a signal generator, a power amplifier (Model AG1010 Amplifier/Generator, T&C Power Conversion Inc., Rochester, NY, USA), a hydrophone (Model HNR-1000, ONDA Corporation, Sunnyvale, CA, USA), a 1 MHz transducer (Hangzhou Applied Acoustics Research Institute, Hangzhou, Zhejiang, China), degassed water, and a water tank. The cylindrical transducer measured 2 cm in diameter and was fixed on a supporter to maintain a distance of 5 cm between the transducer and culture dishes (Figure 1). The center acoustic pressure was adjustable, and the corresponding center spatial-peak,

pulse average (SPPA) intensity was in the 0.4–2.0 W/cm^2 range, calculated with the equation mentioned before. We chose 1.0 W/cm^2 *in vitro* and *in vivo* on the basis of preliminary experimental results. Cell suspensions or tumors were exposed to US for 10 min (duty cycle = 50%). The echo-contrast agent SonoVue (Bracco, Milan, Italy) served as MBs to induce cavitation, measuring 2–8 µm in diameter, and was suspended in 5 mL of sterile saline and shaken thoroughly before use. 2.5×10^8 bubbles per milliliter, on average, were detected. We maintained the MB/cell ratio at around 100/1 in accordance with the study by Pan et al. (Pan et al., 2018).

Databases

The relationship between Piezo1 expression and clinical outcomes in PDAC patients was analyzed based on the following databases: Oncomine, GEO, GEPIA, TCGA, and KM plotter (http://kmplot.com/). Oncomine is a cancer microarray database and web-based data-mining platform that contains differential expression analyses between most major types of cancer and respective normal tissues (Rhodes et al., 2004). GEO is a public functional genomics data repository that contains curated gene expression profiles. GEPIA is an interactive web application for gene expression analysis based on RNA sequencing data of tumors and normal samples from the TCGA and the GTEx databases (Tang et al., 2017). TCGA is a project using genome sequencing and bioinformatics to catalogue genetic mutations responsible for cancer. The Kaplan Meier plotter is a meta-analysis based tool to assess the effect of 54k genes (mRNA, miRNA, protein) on survival in 21 cancer types.

Immunohistochemistry

Immunohistochemical staining was conducted on paraffin-embedded tissues cut into 4 µm sections. The primary antibody for Piezo1 (rabbit, 1:200, Proteintech Cat# 15939-1-AP, RRID:AB_2231460, Chicago, USA) was incubated overnight at 4°C. Subsequently, the antibody was incubated with a biotinylated secondary antibody for 90 min at room temperature and then with an Elite Vectastain avidin–biotin complex–peroxidase kit (1:200, Vector, Cat# PK-6100, Burlingame, CA, USA) for 1 h. Several views were captured on each slide and image J software (ImageJ, RRID: SCR_003070) was used to quantify the area fraction of Piezo1 positive areas.

Immunofluorescence

The cells were incubated with an anti-Piezo1 antibody (rabbit, 1:400, Proteintech Cat# 15939-1-AP, RRID:AB_2231460, Chicago, USA) overnight at 4°C followed by incubation with a secondary antibody conjugated to Alexa Fluor 488 for 1 h at room temperature. The cells were counterstained with wheat germ agglutinin (WGA, Alexa Fluor 555 conjugate, 1:20000, Invitrogen, Cat# W32464, USA) and DAPI (D9542, Sigma, St. Louis, MO, USA) for 5 min.

Western blot analysis

Equal amounts of cell lysates were separated by sodium dodecyl sulfate–polyacrylamide gel electrophoresis before they were transferred onto 0.2 µm or 0.45 µm polyvinylidene fluoride membranes. The primary antibodies used were as follows: rabbit anti-Piezo1 antibody (1:400, Proteintech Cat# 15939-1-AP, RRID:AB_2231460, Chicago, USA), mouse anti-beta actin (1:5000, Abcam Cat# ab8226, RRID:AB_306371, Cambridge, UK), rabbit anti-Cytochrome C (1:1000, Cell Signaling Technology Cat# 11940, RRID:AB_2637071, Danvers, MA, USA), rabbit anti-Bax (1:1000, Cell Signaling Technology Cat# 5023, RRID:AB_10557411, Danvers, MA, USA), and rabbit anti-Bcl-2 (1:1000, Cell Signaling Technology Cat# 3498, RRID:AB_1903907, Danvers, MA, USA).

Apoptosis analysis

By using an apoptosis detection Annexin V–FITC/PI staining kit (BD Bioscience, Cat# 556547, NK, USA), the cells were stained in accordance with the instructions provided by the manufacturer and collected by flow cytometry (BD FACSCanto II, USA). Data were analyzed using the software FlowJo 10.0 (FlowJo, RRID:SCR_008520).

Detection of mitochondrial function

We used a JC-1 staining kit (Beyotime, Cat# C2003S, Shanghai, China) to detect the mitochondrial membrane potential (MMP) (11). For flow cytometry detection, the data collected were analyzed with FlowJo 10.0. Cells that tended to move to the lower right of the scatterplot were cropped and assigned as the

P2 group, representing the percentage of JC-1 monomers. ATP was collected in accordance with the instructions provided by the manufacturer (Xue et al., 2017) and measured with a Multiscan Spectrum (SpectraMax M5, Molecular Device, USA).

Intracellular calcium measurement

Fluo-8 AM (AAT Bioquest, Cat# 21080, Sunnyvale, CA, USA) was used to detect intracellular Ca^{2+} concentration. The work concentration was 5 μM. For fluorescence and flow cytometry detection, data were collected upon cells were expose to ultrasound.

Cell transfection

siRNA duplexes targeting the human Piezo1, negative control (NC), and GAPDH positive control (PC) were synthesized and purified by GenePharma (GenePharma Co., Shanghai, China). RNA oligonucleotides were transfected with Lipofectamine 6000 (Beyotime, Cat# C0526, Shanghai, China); siRNA had a final concentration of 20 μM, and the siRNA (pmol)/Lipo6000™ (μL) ratio was 20/1. Cells were further cultured for another period of 48 h after transfection until they were collected for further assay. For the stable inhibition of Piezo1 expression, the sequence of siRNA was structured to a lentiviral vector (GenePharma Co., Shanghai, China). One NC siRNA and three alternative siRNAs targeting Piezo1 were designed. Green fluorescent protein intensity was used to screen the optimal multiplicity of infection (MOI) and continuous culture time. The optimal MOI was 1/10, and the minimum lethal concentration of puromycin was 0.4 μg/mL. Cells were harvested after continuous culture for 96 h, and the efficiency of transfection was assessed by quantitative polymerase chain reaction and Western blot analysis.

Pancreatic cancer xenografts and treatment

The mice were randomly divided into four groups (Lv-NC, US + MBs + Lv-NC, Lv-siPiezo1, US + MBs + Lv-siPiezo1), with each group consisting of eight mice. Transfected BxPC3 cells (1 x 10^6 cells per mouse) were suspended in sterile phosphate-buffer saline mixed with 1:1 matrigel and then injected subcutaneously into the mice. The Lv-NC group consisted of mice injected subcutaneously with NC siRNA-transfected BxPC3 cells; the US + MBs + Lv-NC group consisted of Lv-NC mice treated using US with MBs; the Lv-si-Piezo1 group consisted of mice injected subcutaneously with Piezo1-targeting siRNA-transfected BxPC3 cells; the US + MBs + Lv-siPiezo1 group included Lv-siPiezo1 mice treated using US with MBs. The tumor weight and tumor volumes (V = 0.5 × L [length] × W^2 [width]) of the mice were measured before each treatment (acoustic intensity = 1.0 W/cm^2; peak negative pressure [PNP] = 176.377 KPa; duty cycle = 50%; exposure time = 10 min; multi-site intratumor administration of 200 μL MBs per mouse). Treatment was administered every other day. On Day 13, the mice were killed, and tissues were harvested. Apoptosis was determined by hematoxylin–eosin (H&E) staining and terminal deoxynucleotidyl transferase-mediated dUTP nick-end labeling (TUNEL) staining (Roche, Cat#11684795910, Basel, Switzerland).

QUANTIFICATION AND STATISTICAL ANALYSIS

Statistical analysis

All data are presented as mean ± SEM. Group comparisons were analyzed using a Student's *t*-test, one-way ANOVA test or two-way ANOVA test, and multiple comparisons were adjusted using the Tukey method. SPSS 23.0 (SPSS, RRID:SCR_002865) and GraphPad Prism 7.0 (GraphPad Prism, RRID:SCR_002798) were used for all statistical analyses. Difference was considered to be significant when p<0.05 (*; #), p<0.01 (**; ##), p<0.001 (***; ###) and p<0.0001 (****; ####).